



A Directed Graph-Based Method for Monitoring and Rapidly Assessing Fire Risk Secondary to Building Earthquakes

Hang Zhang, Baitao Sun, Xiangzhao Chen*

Key Laboratory of Earthquake Engineering and Engineering Vibration Institute of Engineering Mechanics, China Earthquake Administration Key Laboratory of Earthquake Disaster Mitigation, Ministry of Emergency Management, Harbin, Heilongjiang, China

E-mail: chenxz@iem.ac.cn

Abstract. Seismic secondary fires are the main earthquake secondary disasters, and rapid post-earthquake fire risk assessment helps to take effective measures to reduce the occurrence and spread of fires and minimise casualties and property losses. In this paper, a method of monitoring and rapid assessment of earthquake secondary fire risk based on directed graph model is used to determine the fire spread paths between single buildings by on-site investigation and simplified calculation of the buildings in the macro-earthquake epicentre region of the Luding earthquake, and different fire spread partitions by combining with node traversal algorithms to draw a directed graph model of the secondary fire spread in the earthquake in Caiyang Village. By calculating the fire spread risk under 348 fire scenarios and the loss in 71 fire spread zones, it was concluded that the fire spread risk is higher in building nodes 120, 150 and 340, and the fire spread loss is higher in fire spread zones 24, 30, 48, 56, 60, 61, 69 and 71, and it is recommended to strengthen the key fire safety inspection of the above buildings and building zones. Monitoring.

Keywords: Building fire spread monitoring; Directed graphical modelling; Seismic secondary fires; Fire spread risk assessment; Luding earthquake;

1 INTRODUCTION

On 5 September 2022, an earthquake of magnitude Ms6.8 occurred in Luding County, Ganzi Prefecture, Sichuan Province, with many aftershocks. Earthquakes can trigger a series of secondary disasters, and earthquake-induced fires are the secondary disasters

Corresponding author: Xiangzhao Chen, Associate Researcher, PhD, is mainly engaged in the research of seismic hazard risk assessment system (E-mail: chenxz@iem.ac.cn)

Author: Hang Zhang (1998-), Master's Degree Candidate, mainly engaged in the research of disaster prevention, mitigation and protection engineering (E-mail: 3141847560@qq.com).

Baitao SUN (1961-), Researcher, Ph.D., mainly engaged in the research of structural seismic resistance and earthquake hazard science (E-mail: sunbt@iem.ac.cn).

© The Author(s) 2024

B. Yuan et al. (eds.), *Proceedings of the 2024 8th International Conference on Civil Architecture and Structural Engineering (ICCASE 2024)*, Atlantis Highlights in Engineering 33,

https://doi.org/10.2991/978-94-6463-449-5_67

that occur most frequently after earthquakes and cause the most serious disaster losses^[1], and the casualties and economic losses caused by them often exceed those of the earthquake itself^[2].

Himoto proposed a fire spread model for urban buildings based on combustion theory^[3], which proved that there is a positive correlation between the building collapse rate and the building fire start rate in secondary fires from earthquakes^[4]. And more statistical reliability and stability hierarchical Bayesian method is proposed for analysing the secondary fire initiation rate of earthquakes^[5]. Hamada proposed the Hamada model for fire spread in urban buildings through a survey of local buildings in Japan^[6], which yielded that fires spread outwards in an elliptical shape, with the rate of spread being greatest in the downwind direction, followed by the sidewind direction, and least in the upwind direction. Sijian Zhao and Aizhu Ren^[7] analysed the spread mechanism of urban mega fires in depth, constructed a semi-empirical and semi-theoretical model of fire spread, and proposed that the main modes of fire spread are thermal radiation, thermal plume and flying fire. Simplified simulation of fire spread between urban buildings was carried out. Since the monitoring and assessment of secondary fire risk from earthquakes is an important disaster prevention and mitigation emergency work, which requires rapid access to information on earthquake-hit areas and rapid assessment, this paper is based on the simplified assessment method of fire spread risk proposed by Fei-Yang Zheng^[8].

2 OVERVIEW OF THE MACRO-EARTHQUAKE EPICENTRE REGION OF THE LU DING EARTHQUAKE

The study area of this paper is Caiyang Village in Moushi Town, with a total of 348 single buildings in the village, mainly including three categories of self-built masonry structure, pierced wooden structure and bottom frame structure, as shown in Fig 1. According to the on-site investigation data, most of the single buildings in Caiyang Village are between 1~3 storeys, with the height of the first storey being 3.3m, and the height of the second storey and above being 3 m. The opening of the buildings is mostly 3 rooms, and some of the buildings are 4~6 rooms, with the length of the unit opening being 3.6 m. Most of the buildings are built with wooden roof, and the single-storey buildings and the two-storey buildings are mostly built with wooden partitions, and the doors and windows are mostly built with wooden overhanging beams. The bottom of the sub-frame structure is used as a shop, and the superstructure is used for storage and residence, which may store a large number of flammable items.

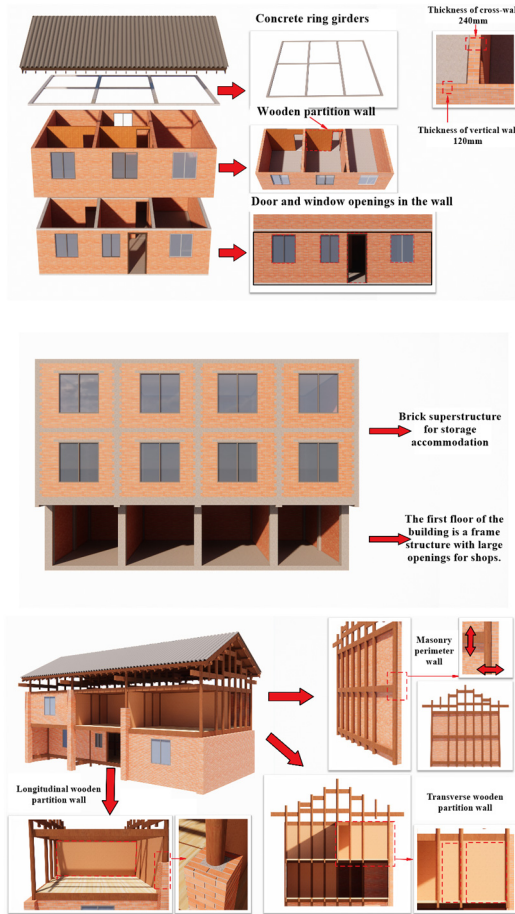


Fig. 1. Typical building types

In order to quickly obtain the building plan location information at the earthquake site, the images taken at the site by the UAV were used, combined with the location coordinates of various types of buildings, and the ArcGIS software was used to draw the building plan layout map, as shown in Fig.2.



Fig. 2. Layout of buildings in the macro-earthquake area

3 ANALYSIS OF THE PATH OF SPREAD OF FIRES SECONDARY TO EARTHQUAKES

In order to meet the timeliness requirements for the assessment of fires secondary to earthquakes, fire spread paths should be assessed by methods that are as simple and rapid as possible. This paper refers to the method of NFPA 80A to determine the fire spread path, and divides the situation of post-earthquake building plan distribution in Caiyang Village into adjacent and spaced arrangements, and classifies the building fire spread risk into the following four cases according to the presence or absence of fire-resistant construction measures as shown in Table 1.

Table 1. Risk profile of building fire spread

	adjacent	spaced arrangements
Lack of fire-resistant structural measures	Scenario 1	Scenario 2
Perfect fire prevention construction measures	Scenario 3	Scenario 4

3.1 Scenario 1

In this earthquake, in Caiyang Village, there were a large number of penetrating wooden buildings with poor fire resistance, and the buildings were filled with earthquake-damaged building collapses, as well as ideal fuels for the spread of fire. In this case, it is considered that no fire-resistant construction measures were installed between the buildings, and that the buildings were able to ignite each other, with a two-way path of spreading^[9].

3.2 Scenario 2

Buildings are arranged in close proximity to each other and have good fire-resistant construction measures. If the fire-resistance limits of the fire-resistant construction measures between buildings located in close proximity to each other meet the requirement of being able to withstand the duration of the fire, it is assumed that the path of fire spread between the buildings does not exist.

3.3 Scenario 3

In this case, the effects of both thermal plume and thermal radiation on the spread of fire between buildings are considered^[10]. The minimum safe distances between buildings under thermal plume are shown in Table 2.

Table 2. Minimum fire safety distances for neighbouring buildings under the influence of a thermal plume

Number of floors with fire	Horizontal or vertical distance
1	7.5m
2	10m
3	12.5m

The minimum safe distance between buildings under the action of thermal radiation is calculated using the formula 1.

$$q_r = \frac{2I_0\lambda}{\pi} \left[\frac{x}{\sqrt{x^2 + y^2}} \arctan\left(\frac{z}{\sqrt{x^2 + y^2}}\right) + \frac{z}{\sqrt{y^2 + z^2}} \arctan\left(\frac{x}{\sqrt{y^2 + z^2}}\right) \right] \quad (1)$$

Where: y is the distance between the emitting and receiving surfaces of thermal radiation, q_r is the amount of radiation received by the surface source, for the wooden components in the building, the study considered that the frontal critical amount of thermal radiation received takes the value of 12.5kw/m^2 and when $q_r > 12.5\text{kw/m}^2$, it is considered that the building will be ignited. I_0 is the intensity of the radiation source, taking the fire temperature as $1,059^\circ\text{C}$, which I_0 corresponds to 178.6kW/m^2 , x takes the value of the half of the building height, z takes the value of the half of the value of the building width of the horizontal walls, λ is the value of the opening ratio of the external walls of the building as the source of the fire. The opening rate of the external wall is taken as the fire source.

Based on the information from the site investigation, the structural opening rate and the total building minimum safety distance were calculated for a self-built masonry structure as an example, and the results are shown in Table 3 and Table 4.

Table 3. Rate of openings in self-built masonry structures

No. of floors	Building heights	Front longitudinal wall opening rate	Rear longitudinal wall opening rate
1	3.3m	40%	12%
2	6.3m	37.5%	23.5%
3	9.3m	36.7%	27.3%

Table 4. Minimum safe distance for self-built masonry structures

Building openings	Length of opening	No. of floors	Minimum safe distance to front wall	Minimum safe distance to rear wall
1	3.6	1	4.3	1.7
		2	5.5	4.0
2	7.2	1	5.8	2.1
		2	7.9	5.8
3	10.8	1	6.8	2.2
		2	9.6	7.0

When the location of the fire-starting building is lower than that of the spacing building, the minimum safe distance is determined by taking the maximum value of the thermal radiation and thermal plume calculations. When the location of the fire-starting building is higher than or equal to that of the spacing building, only the effect of thermal radiation on the spread of the fire is taken into account, and the minimum distance is determined in accordance with the calculation of the amount of thermal radiation received and in accordance with the critical thermal radiation flux.

3.4 Scenario 4

The buildings are arranged at intervals with good fire construction measures. In this case, if the relative directions of the buildings are not roughly pressed in the window and door openings, it is considered that there is no fire spread path between the two buildings.

4 EARTHQUAKE SECONDARY FIRE SPREAD DIRECTIONAL MAP MODELLING

In order to determine the fire spread relationship, a single building is regarded as a node in a directed graph, and the fire spread relationship is regarded as a directed edge of a node, so as to establish a directed graph model of the fire spread in the study area, and the network of directed graphs formed by a large number of nodes X and directed edges Y is denoted as $F_{fire} = (X, Y)$, and the adjacency and spread matrices are used to describe the fire spread relationship and the fire spread range among the nodes^[11]. In order to determine the ignition relationship between fire-starting nodes and adjacent buildings, it is necessary to determine the fire spread path between different buildings. There are 348 buildings in the study area of this paper, and the node locations and numbers are shown in Fig. The value of the neighbourhood matrix is shown in formula 2:

$$F_{road}(i, j) = \begin{cases} 1, i \neq j, (x_i, x_j) = 1 \\ 0 \end{cases} \quad (2)$$

The significance of $(x_i, x_j) = 1$ is the existence of directed edges between node x_i and node x_j , $F_{road}(i, j) = 1$ means that there is a seismic secondary fire spread path between building i and building j , and $F_{road}(i, j) = 0$ means that there is no seismic secondary fire spread path between building i and building j .

The establishment of the adjacency matrix is divided into two steps, one is to calculate the fire spreading path between nodes and obtain the adjacency vector of each node, and the second is to combine the vectors into the adjacency matrix, and then obtain the spreading relationship of the whole network, taking Caiyang Village No. 2 spreading

sub-district as an example, and the establishment of the adjacency matrix is shown in Fig. 3.

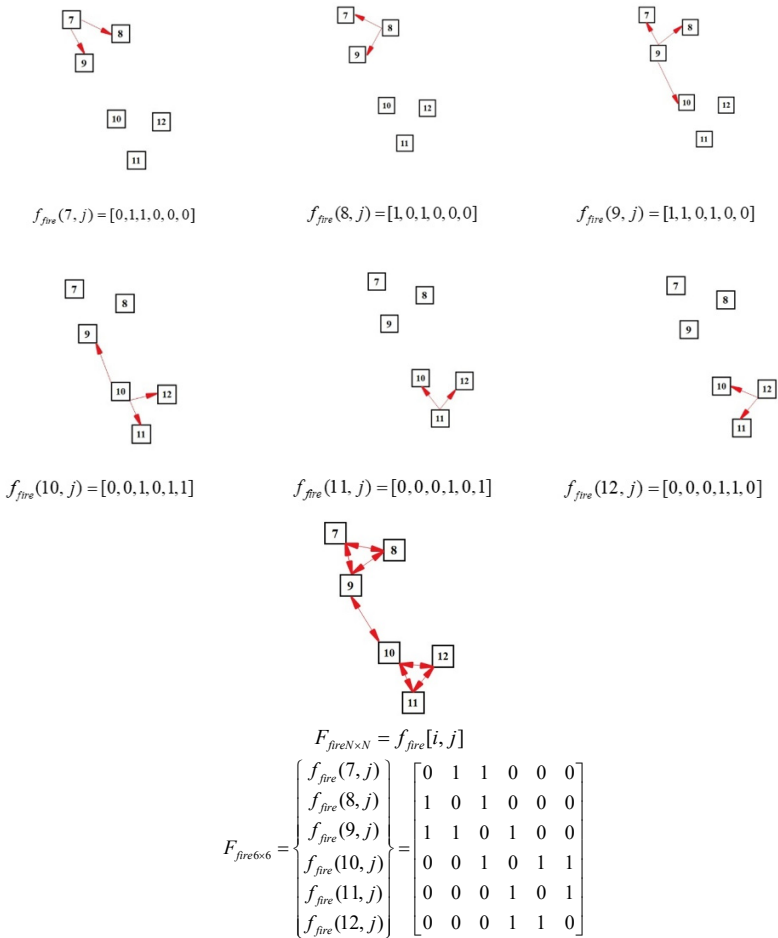


Fig. 3. Process of building the adjacency matrix

According to the above method to obtain the fire spread directed graph model is shown in Fig. 4.

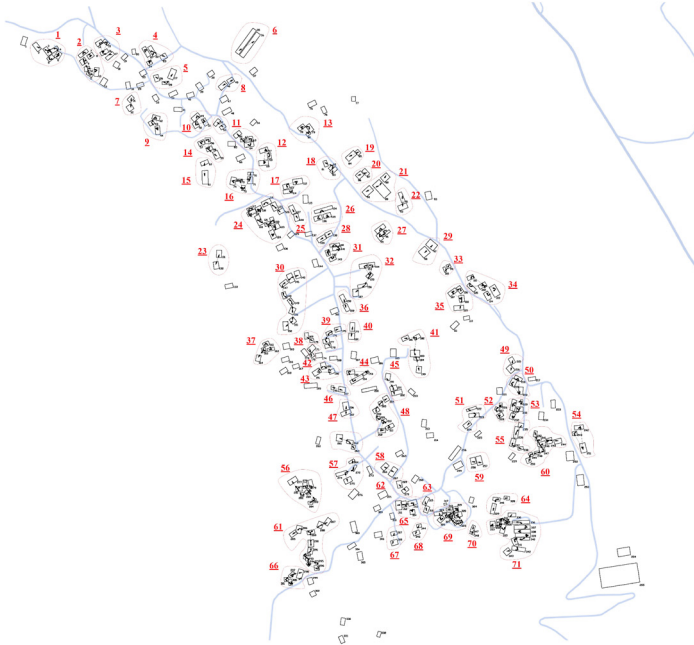


Fig. 4. Directional map model of fire spread secondary to earthquake in Caiyang village

5 RISK ANALYSIS OF THE SPREAD OF FIRES SECONDARY TO EARTHQUAKES

5.1 Analysis of fire spread scenarios secondary to earthquakes

The node traversal algorithm is used to determine the maximum area that may be affected by fire node x_i by visiting all the nodes in the directed graph that are connected to fire spreading paths with fire node x_i when only 1 initial node is considered to be on fire. The specific steps of the node traversal algorithm are as follows:

1. Construct seismic secondary fire spread contribution matrix name as $A_i=0$, let the traversal number $k=1$, assuming that the fire building node is x_i ;
2. Starting the traversal at the fire-starting building node x_i , the set of nodes that satisfy the node value of $F_{fire}(i, j)$ in row i of its adjacency matrix $f_{fire}(i, j)=1$ is recorded as the ignited set J ;
3. Let the fire spread contribution matrix recording the ignited node column number j be $A(k, j)=j$;
4. Let the element of column j in the adjacency matrix $F_{fire}(i, j)$ be 0;

5. Increased number of traversals $k = k + 1$;
6. Let the nodes in the ignited set J be traversed as fire source nodes, exclude the ignited node numbers, and repeat steps 1.2.3.4.5, until $J = \emptyset$;

Taking node 9 in Fig. 4 as an example, the fire spread contribution matrix is calculated $A_9(7,8,10,11,12) = \begin{pmatrix} 0 & 0 & 11 & 0 & 0 \\ 0 & 0 & 12 & 0 & 0 \end{pmatrix}$, To determine the order of fire initia-

tion at building nodes ignited by the fire source node, the seismic secondary fire spread order matrix B_i is constructed, where the rows of matrix B_i represent the

rounds of fire spread in which it was ignited, $B_9 = \begin{pmatrix} 7 & 8 & 10 \\ 11 & 12 \end{pmatrix}$. The elements of the

earthquake secondary fire spread order matrix are generalised to form a set of ignitable nodes, denoted as set $C_i, C_9 = (7 \ 8 \ 10 \ 11 \ 12)$. In order to describe the im-

impact of different inter-building fires on the surrounding buildings, the seismic secondary fire spread impact matrix $D_{m \times m}$ is constructed to indicate whether the building node will eventually be ignited by a building node after a fire starts in that building node. Its matrix elements are shown in formula 3.

$$D_{i,j} = \begin{cases} 1, & j \in C_i \\ 1, & i = j \\ 0, & j \notin C_i \end{cases} \tag{3}$$

In order to describe the impacts of different inter-building fires on the surrounding buildings, a matrix of secondary fire spreading impacts of earthquakes was constructed $D_{m \times m}$. Based on the fire spreading relationship between single buildings, the whole study area was divided into 71 spreading partitions, as shown in Fig. 4.

5.2 Analysis of fire losses secondary to earthquakes

Summing the elements of the earthquake secondary fire spread impact matrix yields the number of spreading building losses L_i caused by a particular fire building node x_i , as shown in formula 4.

$$L_i = \sum_{j=1}^m D_{i,j} \tag{4}$$

The building loss expectancy can be used to measure the ability of a building to withstand a fire secondary to an earthquake after an earthquake has occurred. Let the spreading building loss expectation due to a fire at building node i be $E(L)_i$, as shown in Equation 5.

$$E(L)_i = L_i P_i \tag{5}$$

P_i is the probability of the occurrence of the node of the burning building in this spreading scenario, which is the same everywhere in the study area, with a total number of 348 buildings, hence $P_i = 1/348$. For a group of buildings totalling 348 in the entire

study area after the earthquake, the building loss expectation is: $E = \sum E(L)_i = \sum_{i=1}^{348} L_i P_i$

After the earthquake secondary fire, the fire spread region between single buildings is divided into 71 regions as described in the previous section, and the loss of the spread region is taken as the maximum value of each spread loss scenario in the region, and the loss expectation value is the sum of the loss of each spread region scenario. According to the above formula, 348 fire spread scenarios and losses in 71 spread regions in the Caiyang Village earthquake secondary fire spread directed graph model are obtained, as shown in Fig. 5. It was assessed that the scope of fire spreading after the earthquake secondary fire in buildings 120, 150 and 340 in Caiyang Village was larger, and that the risk of fire spreading in the areas of 24, 30, 48, 56, 60, 61, 69 and 71 was much greater than that in the other areas, and that the focus should be on the fire prevention of the above-mentioned buildings and areas after the earthquake, so that hidden dangers could be detected in a timely manner and measures taken to eliminate them.

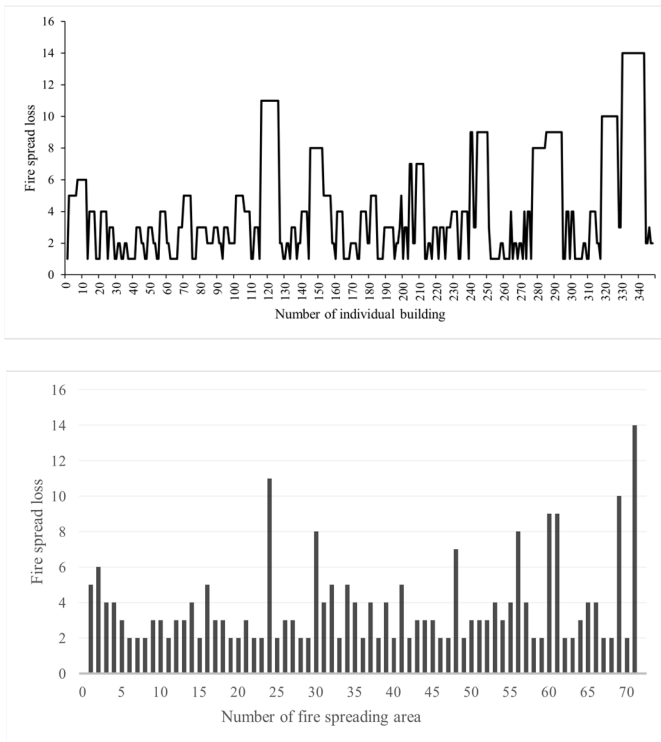


Fig. 5. Caiyang Village earthquake secondary fire spread damage by scene and area

6 CONCLUSIONS

In this paper, a rapid assessment of the secondary fire risk of the Luding earthquake was carried out based on a directed graphical model, combined with the information from the site investigation. It is capable of meeting the requirements for rapid access to information on earthquake-hit areas and rapid assessment in disaster prevention and mitigation emergency response.

Although this study provides an effective method for monitoring and rapid assessment of secondary fire risk after building earthquakes, there are still some limitations. Firstly, local temperature and humidity, weather precipitation, wind speed and direction, and buildings containing explosive materials were not considered, and secondly, the fire spreading paths only existed in the case of spreading and non-spreading, and combustible materials were not considered in the case of cloudy combustion, which may affect the accuracy of the assessment results. Therefore, future research can consider the above factors and introduce the concept of fire spread probability to further optimise the model parameters and improve the data collection mechanism in order to improve the accuracy and reliability of the assessment.

ACKNOWLEDGMENT

Funding from the Key R&D Plan of Heilongjiang Province [grant numbers GA22C001] and Scientific Research Fund of Institute of Engineering Mechanics, China Earthquake Administration (Grant No. 2021EEEEVL0203) .

REFERENCES

1. ZHONG Jiangrong, WANG Qi, LIN Xuchuan. Study on the spread model of urban secondary fire induced by earthquake [J]. World Earthquake Engineering, 2024, 40(1): 49–57. DOI:10.19994/j.cnki.WEE.2024.0005.
2. ZHONG Jiangrong. Study on the Seismic secondary fires Disaster in the Urban [D/OL]. Institute of Engineering Mechanics, China Earthquake Administration, 2010[2024–04–09].
3. Anonymous. Proceedings: u.s.-japan workshop on urban earth-quake hazards reduction, held at stanford university, july 29-august 1, 1984[M]. EERI, 1985.
4. HIMOTO K, TANAKA T. A physically-based model for urban fire spread[J]. Fire Safety Science, 2003, 7: 129–140. DOI:10/bznhxx.
5. HIMOTO K. Hierarchical bayesian modeling of post-earthquake ignition probabilities considering inter-earthquake heterogeneity[J]. Risk Analysis, 2020, 40. DOI:10/gtqj9s.
6. YOSHIOKA H, HIMOTO K, KAGIYA K. Large urban fires in japan: history and management[J]. Fire Technology, 2020, 56(5): 1885–1901. DOI:10/gtqk6k.
7. ZHAO Si-jian, XIONG Li-ya, REN Ai-zhu. The GIS-based Simulation of Urban Mass Fire Spread [J]. FIRE SAFETY SCIENCE, 2006(3): 128-137+2.
8. ZHENG Fei-yang, ZHANG Liang, SONG Zhi-gang, Simplified assessment method of fire spread risk of village buildings based on network model [J]. Fire Science and Technology, 2022, 41(4): 496–500.

9. NFPA 914 code development[EB/OL](2019). <https://www.nfpa.org/codes-and-standards/nfpa-914-standard-development/914>.
10. NFPA 80a standard development[EB/OL](2017). <https://www.nfpa.org/codes-and-standards/nfpa-80a-standard-development/80a>.
11. ZHANG Jian, SONG Zhi-gang, LI Quan-wang. Identification and fire protection evaluation of critical buildings to prevent fire spread in densely built wood building areas [J]. Engineering Mechanics, 2020, 37(4): 60–69.

Open Access This chapter is licensed under the terms of the Creative Commons Attribution-NonCommercial 4.0 International License (<http://creativecommons.org/licenses/by-nc/4.0/>), which permits any noncommercial use, sharing, adaptation, distribution and reproduction in any medium or format, as long as you give appropriate credit to the original author(s) and the source, provide a link to the Creative Commons license and indicate if changes were made.

The images or other third party material in this chapter are included in the chapter's Creative Commons license, unless indicated otherwise in a credit line to the material. If material is not included in the chapter's Creative Commons license and your intended use is not permitted by statutory regulation or exceeds the permitted use, you will need to obtain permission directly from the copyright holder.

